ChemComm

Accepted Manuscript

This article can be cited before page numbers have been issued, to do this please use: B. Coulson, M. Issacs, L. Lari, R. E. E. Douthwaite and A. Duhme-klair, *Chem. Commun.*, 2019, DOI: 10.1039/C9CC02197C.

ROYAL SOCIETY OF CHEMISTRY

rsc.li/chemcomm

View Article Online
DOI: 10.1039/C9CC02197C

COMMUNICATION

Carbon Nitride as a Ligand: Edge-Site Coordination of $ReCl(CO)_3$-fragments to g-C_3N_4

Received 00th January 20xx,
Accepted 00th January 20xx

DOI: 10.1039/x0xx00000x

Ben Coulson,[a] Mark Isaacs,[b] Leonardo Lari,[c] Richard E. Douthwaite*[a] and Anne-K. Duhme-Klair *[a]

Direct coordination of $ReCl(CO)_3$-fragments to carbon nitride (g-C_3N_4) occurs via κ^2 *N*, *N*' bidentate coordination at edge sites, and IR spectroscopy of the carbonyl bands suggests that for $ReCl(CO)_3$, g-C_3N_4 acts as ligand donor comparable to a glyoxime.

The attachment of soluble metal complexes to a solid support is a powerful strategy to combine the advantages of solution and solid phase chemistry. For example, flow chemistry and catalysis can benefit from a well-defined metal environment to control activity and selectivity, which can be combined with simple product separation, characteristic of an heterogeneous system.[1] The immobilisation of metal complexes on solid supports is achieved using various methods, ranging from simple adsorption to covalent linking of the metal complex to the solid support.[1-2] The most common solid supports by far are metal oxides, but also metal halides and carbonaceous materials have been investigated intensively. Of the latter class of materials, carbon nitrides, primarily graphitic carbon nitride (g-C_3N_4) have been of interest, as supports and catalysts for light-driven redox catalysis.[3]

Structurally, g-C_3N_4 is characterised by repeating heptazine moieties, which are condensed into chains and sheets, depending on the synthesis conditions (Scheme 1).[4] The structure of g-C_3N_4 contains potential metal coordination sites similar to motifs of *N*-heterocyclic ligands, both internally and at edge sites (Scheme 1). Indeed the addition of metal ions and atoms has been studied for a range of applications, although in most cases detailed structural understanding of metal coordination is limited due to the challenging characterisation of these complex materials.[5] Metal complexes have also been anchored to g-C_3N_4 using covalent linkers.[3c, 6]

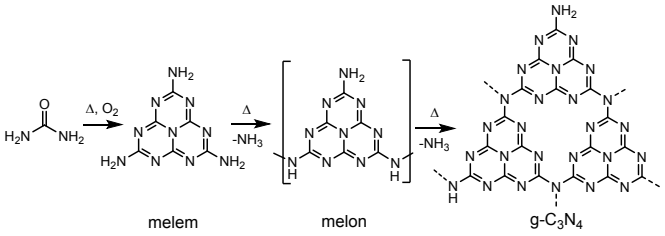

Scheme 1. Structural motifs of carbon nitride arising from sequential condensation steps

We were motivated to study the direct coordination of functional metal complex fragments to g-C_3N_4 with the ultimate aim of studying light-driven and thermal catalytic applications that may benefit from the established photoactivity and acid/base behaviour of g-C_3N_4. Herein we describe the addition of $ReCl(CO)_3$ moieties to g-C_3N_4 and the characterisation of the resulting material. Known molecular derivatives, such as $[ReCl(bpy)(CO)_3]$ (bpy = 2, 2'-bipyridine) have attracted interest for artificial photosynthesis and for the catalytic photoreduction of CO_2.[7] Subsequent studies have found that the replacement of bipyridine with, bulkier *N*-donor ligands results in more stable active catalysts, because the steric bulk of the ligand prevents the formation of catalytically-inactive dimers.[7b, 8] The distinct vibrational frequencies of the carbonyl ligands allow their use as 'reporter' ligands for the identification of catalytically-relevant carbonyl species using IR and Raman spectroscopy.[9]

Steric considerations of g-C_3N_4 structural motifs (*vide infra*) suggest that the direct coordination of metal complexes to g-C_3N_4 is most likely to occur at the edge sites of g-C_3N_4 (Scheme 1), which contain both pyridyl and amino moieties. In addition, to model direct coordination to g-C_3N_4, we have also investigated coordination to the commercially available ligand 5, 7-dimethyl-[1, 8]-naphthyridin-2-amine (DMNA) (Scheme 2), which contains a similar structural motif and hence has been chosen as a model for g-C_3N_4 binding mode(s).[10]

[a] Department of Chemistry, University of York, York, YO10 5DD, UK. Email:richard.douthwaite@york.ac.uk
[b] HarwellXPS, R92 Research Complex at Harwell, Rutherford Appleton Laboratories, Harwell, Didcot, OX11 0QS, UK, and Department of Chemistry, University College London, 20 Gordon Street, London, WC1H 0AJ, UK.
[c] Department of Physics, University of York, Heslington, York, YO10 5DD, UK.
† Electronic Supplementary Information (ESI) available: Experimental details and additional characterisation of all compounds and materials. CCDC 1897421. See DOI: 10.1039/x0xx00000x

The preparation of g-C_3N_4 was achieved using a literature procedure *via* the thermal degradation of urea (see experimental section in the ESI†).[11] Characterisation by powder X-ray diffraction (PXRD), elemental analysis, solid state ^{13}C NMR and scanning electron microscopy (SEM) (see details in the ESI†) is consistent with that reported for g-C_3N_4 comprised primarily of the melon structural motif (Scheme 1). The reaction between $[ReCl(CO)_5]$ and g-C_3N_4 in toluene at 80 °C gave $[ReCl(CO)_3(g\text{-}C_3N_4)]$ as a yellow solid. PXRD of $[ReCl(CO)_3(g\text{-}C_3N_4)]$ (Fig. S1, ESI†) shows broad peaks at 13.1 and 27.4° 2θ, corresponding to an interlayer spacing of 0.325 nm for the aromatic heptazine units.[12] The data are indistinguishable from g-C_3N_4 indicating that intercalation of a metal complex has not occurred. A comparison of the SEM images of $[ReCl(CO)_3(g\text{-}C_3N_4)]$ with those of g-C_3N_4 (Fig. S2, ESI†) confirms that the reaction with $[ReCl(CO)_5]$ does not significantly change the morphology of g-C_3N_4. The rhenium loading of $[ReCl(CO)_3(g\text{-}C_3N_4)]$ was determined by ICP-MS and chlorine loading by combustion analysis, giving 7.35 and 1.17 wt %, respectively, which indicates a Re : Cl ratio of 1:0.85.

X-ray photoelectron spectroscopic (XPS) characterisation of $[ReCl(CO)_3(g\text{-}C_3N_4)]$ and g-C_3N_4 produced very similar N 1s spectra (Fig. S3a and b, ESI†), consistent with urea-derived g-C_3N_4.[13] In contrast, the C 1s spectra show significant differences with an additional signal at 286.6 eV observed for $[ReCl(CO)_3(g\text{-}C_3N_4)]$, consistent with carbonyl ligands (Fig. 1a and b).[14] The Re 4f spectrum of $[ReCl(CO)_3(g\text{-}C_3N_4)]$ (Fig. S3c, ESI†) shows two peaks at 42.2 and 44.6 eV, fitted to Re $4f_{7/2}$ and $4f_{5/2}$ signals, respectively. The peak width (fwhm = 1.25 eV) and binding energies are consistent with a single rhenium(I) environment.[15]

Collectively, the PXRD and XPS data indicate that the coordination of the rhenium moiety most likely occurs at the edge sites of g-C_3N_4. The insolubility of g-C_3N_4 presents challenges for the direct determination of the exact metal coordination environment. Hence, to model the coordination of metal fragments to g-C_3N_4, the commercially available ligand, 5, 7-dimethyl-[1 ,8]-naphthyridine-2-amine (DMNA) was selected, because DMNA contains both [1, 8]-naphthyridine and primary amine functionalities, analogous to the heptazine moieties at the edges of g-C_3N_4. Comparison of the characterisation data, in particular the infrared spectra (*vide infra*) of $[ReCl(CO)_3(g\text{-}C_3N_4)]$ and $[ReCl(CO)_3(DMNA)]$, could provide insight into the coordination modes. Reported DMNA complexes exhibit a range of binding motifs including monodentate *N*-heterocyclic,[16] κ²-*N*, *N'*-heterocyclic,[16-17] and κ³ *N*, *N'*, *N''*-heterocyclic/amido coordination.[18]

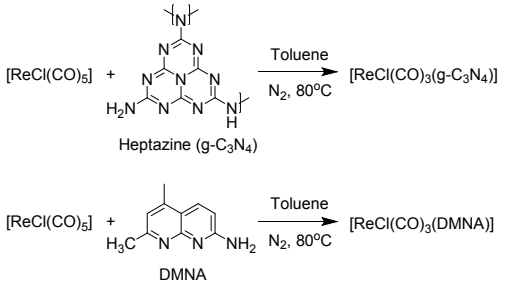

Scheme 2: Synthesis of $[ReCl(CO)_3(g\text{-}C_3N_4)]$ and $[ReCl(CO)_3(DMNA)]$.

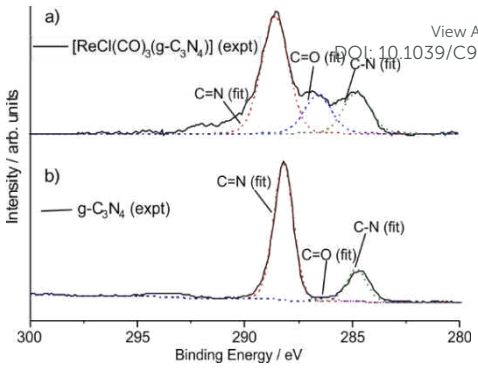

Fig. 1 XPS spectra a) C 1s $[ReCl(CO)_3(g\text{-}C_3N_4)]$; b) C 1s g-$C_3N_4$.

Reaction between $[ReCl(CO)_5]$ and DMNA in toluene at 80 °C gave $[ReCl(CO)_3(DMNA\text{-}\kappa^2 N, N')]$ (Scheme 1). ^1H and ^{13}C NMR, mass spectrometry, and elemental analysis data are consistent with the proposed formulation (see ESI†). A single crystal diffraction study of $[ReCl(CO)_3(DMNA\text{-}\kappa^2 N, N')]$ confirms the formulation and the molecular structure (Fig. 2). The geometry about the rhenium atom is *pseudo*-octahedral with facial carbonyl ligands, as commonly observed for complexes of $ReCl(CO)_3(NN)$ (where NN = bidentate *N*-donor ligand). The DMNA ligand is coordinated to rhenium *via* both [1, 8]-naphthyridineyl nitrogen atoms N1 and N2, whilst the adjacent amine group is uninvolved in metal coordination. This binding mode is also observed for several other DMNA complexes including $[MCl_2(DMNA)_2]$ (where M = Mn, Co and Ni). [17b-d]

For $[ReCl(CO)_3(DMNA)]$, the Re-N bond lengths are 2.212(2) and 2.218(2) Å, compared to 2.168(7) and 2.173(8) Å, respectively, for $[ReCl(bpy)(CO)_3]$.[19] The N1-Re1-N2 bite angle of $[ReCl(CO)_3(DMNA)]$ is 60.41(8)°, which lies within the range 54.6-62.6° found for other κ² *N, N'* complexes of DMNA, but as expected, is smaller than observed for $[ReCl(bpy)(CO)_3]$ (74.6(3)°). Other metrical data are enumerated in the ESI†.

Comparison of the IR spectra of g-C_3N_4, $[ReCl(CO)_3(g\text{-}C_3N_4)]$, and $[ReCl(CO)_3(DMNA\text{-}\kappa^2 N, N')]$ allow the identification of carbonyl-containing metal fragments and support structural assignment. The solid state ATR-IR spectra of g-C_3N_4 and $[ReCl(CO)_3(g\text{-}C_3N_4)]$ (Fig. S4, ESI†) show that the bands assigned

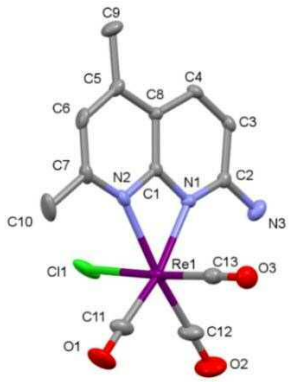

Fig. 2 Molecular structure of $[ReCl(CO)_3(DMNA\text{-}\kappa^2 N, N')]$. Thermal ellipsoids are at 50 % probability level and hydrogen atoms have been omitted for clarity.

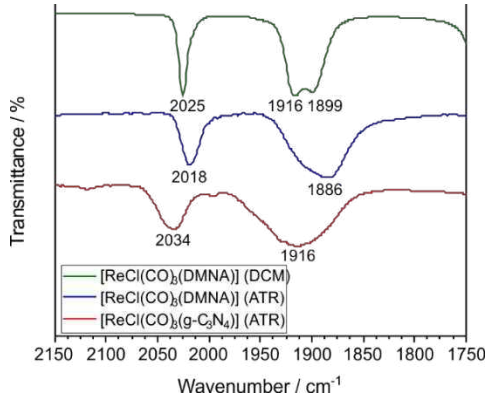

Fig. 3 Infrared spectra of $[ReCl(CO)_3(g\text{-}C_3N_4)]$ and $[ReCl(CO)_3(DMNA)]$.

Table 1 Infrared spectroscopic data associated with $[ReCl(CO)_3(g\text{-}C_3N_4)]$ and related compounds.

Material (IR mode)	ν_{CO} / cm^{-1}
$[ReCl(CO)_5]$ (solution, DCM)	1986, 2047
$[ReCl(CO)_3(DMNA)]$ (solution, DCM)	1899, 1916, 2025
$[ReCl(CO)_3(bpy)]$(solution, DCM)[9a]	1899, 1921, 2024
$[ReCl(CO)_3(DMNA)]$ (ATR)	1886 (br), 2018
$[ReCl(CO)_3(g\text{-}C_3N_4)]$ (ATR)	1916 (br), 2034

to carbon nitride are unchanged as a result of metal complex coordination, presumably due to the low loading. Nevertheless, $[ReCl(CO)_3(g\text{-}C_3N_4)]$ shows strong vibrational bands in the carbonyl region, with a broad band centred at 1916 cm^{-1} and a sharper band at 2034 cm^{-1}. Using diffuse reflectance infrared Fourier transform spectroscopy (DRIFTS) (Fig. S5, ESI†), which has higher surface sensitivity, the metal-carbonyl vibrational band intensity increases compared to g-C_3N_4, indicating that the carbonyl-containing species is concentrated at the surface, which is consistent with the PXRD and XPS data.

The solution IR spectrum of $[ReCl(CO)_3(DMNA\text{-}\kappa^2\ N,\ N')]$ in dichloromethane (Fig. 3) shows three carbonyl bands at 1899, 1916 and 2025 cm^{-1}, respectively, as expected for an octahedral rhenium tricarbonyl species with facial geometry, assigned to the totally symmetric in-phase A'(1) vibration, the equatorially asymmetric A'' and totally symmetric out-of-phase A'(2) modes, respectively.[9b, 20] These data can be compared to other complexes containing bidentate nitrogen ligands including $[ReCl(bpy)(CO)_3]$, which show bands at very similar frequencies (Table 1), suggesting that the ligand donor properties of bpy and DMNA are very similar.[9a] In the solid state, the vibrational bands of $[ReCl(CO)_3(DMNA\text{-}\kappa^2\ N,\ N')]$ broaden, causing an overlap of the two lower energy bands observed in solution and all bands are shifted to lower energy by 6-13 cm^{-1} (Table 1). For $[ReCl(CO)_3(g\text{-}C_3N_4)]$, comparing the number and position of CO vibrational bands with the precursor $[ReCl(CO)_5]$ confirms that simple physisorption of $[ReCl(CO)_5]$ onto g-C_3N_4 has not occurred; instead the data are consistent with direct coordination. Due to the insolubility of $[ReCl(CO)_3(g\text{-}C_3N_4)]$ in common solvents, a solution IR spectrum of $[ReCl(CO)_3(g\text{-}C_3N_4)]$ could not be obtained. However, in the solid state the number and shape of the CO bands of $[ReCl(CO)_3(g\text{-}C_3N_4)]$ resemble those of $[ReCl(CO)_3(DMNA\text{-}\kappa^2\ N,\ N')]$, thereby indicating that a facial (*fac*) $Re(CO)_3$ moiety is present in $[ReCl(CO)_3(g\text{-}C_3N_4)]$ (Fig. 3). The higher energy carbonyl bands of $[ReCl(CO)_3(g\text{-}C_3N_4)]$ compared to those of $[ReCl(CO)_3(DMNA\text{-}\kappa^2\ N,\ N')]$ reveal a lower electron density at the metal centre, suggesting either that g-C_3N_4 donates less electron density than the DMNA ligand, or that g-C_3N_4 is a very strong π-acceptor. To investigate the ligand properties and binding strength of g-C_3N_4 further, $[ReCl(CO)_3(g\text{-}C_3N_4)]$ was stirred for 3 hours in solvents of varying metal-coordinating ability, followed by centrifugation and subsequent IR analysis of both the supernatant and the solid residue (Fig. S6 and S7, ESI†). The IR spectra show that in strongly-coordinating solvents, such as MeCN and ethanol, significant leaching occurs, indicating that g-C_3N_4 is a weak donor ligand. Other $ReCl(CO)_3$ complexes with common *N*-donor ligands such as triazole,[21] imidazole,[22] and imines,[23] show carbonyl bands at lower energies broadly similar to those obtained for $[ReCl(bpy)(CO)_3]$ (Table 1). However, similar CO band positions are observed for the weak κ^2 *N, N'* donor ligand dimethylglyoxime (DMG), in the complex $[ReCl(CO)_3(DMG)]$ which exhibits CO bands at 2032, 1938, 1916 cm^{-1},[24] similar to those of $[ReCl(CO)_3(g\text{-}C_3N_4)]$ (Table 1).

Collectively, the data suggest that direct coordination of metal complex fragments to g-C_3N_4 can occur, with g-C_3N_4 acting as a bidentate *N*-donor ligand. Spectroscopic evidence and the leaching observed in coordinating solvents indicate that g-C_3N_4 is a weak donor with electronic properties that resemble those of a bidentate glyoxime ligand. On a solid support, steric interactions between the support and a metal complex moiety will be significant. Comparison between the size of a $ReCl(CO)_3$ moiety (ca. 0.55 nm diameter), estimated from the crystal structure of $[ReCl(CO)_3(DMNA\text{-}\kappa^2 N,\ N')]$, and the interplanar distance of 0.325 nm for g-C_3N_4, determined from PXRD, suggest $ReCl(CO)_3$ could only bind to exposed edge sites. Non-covalent interactions will likely prevent coordination at plane edge sites of g-C_3N_4 with coincident plane termination or stepped planes (Fig. 4).

To directly image and analyse the distribution of $ReCl(CO)_3$ moieties in $[ReCl(CO)_3(g\text{-}C_3N_4)]$, (Scanning)Transmission Electron Microscopy (S)TEM with Energy Dispersive X-ray (EDX) was used High Angle Annular Dark Field (HAADF) imaging (Fig. 5 and Fig. S9, ESI†) shows the concentration of bright features along edges of g-C_3N_4 particles, and EDX (Fig. S10, ESI†) shows that Re and Cl are co-located in these regions. At the greatest magnification (Fig. S11, ESI†), some isolated bright features 200 pm in diameter can be identified, which are larger than

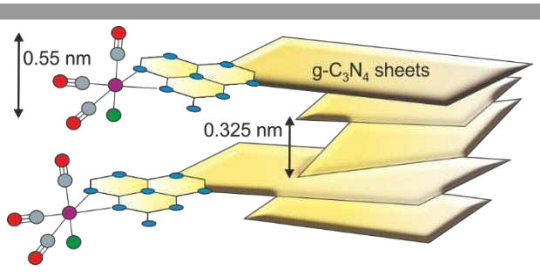

Fig. 4. Illustration of $ReCl(CO)_3$ coordination to g-C_3N_4.

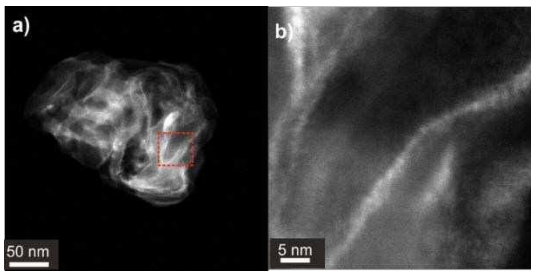

Fig. 5. a) HAADF image of [ReCl(CO)$_3$(g-C$_3$N$_4$)]. Bright areas correspond to location of Re and Cl; b) higher magnification of the region within the red box of a)

individual atoms but could be consistent with Re-Cl moieties.

In conclusion, direct coordination of metal complex fragments to bidentate *N*-donor edge sites represents an additional functionalisation strategy of g-C$_3$N$_4$, in addition to intraplanar metal ion/atom coordination, and anchoring *via* a covalent linker. Notwithstanding the relatively weak binding observed for ReCl(CO)$_3$, there is an opportunity to develop new classes of multifunctional materials comprising metal complex/g-C$_3$N$_4$ composites that can exploit, for example, the photophysical and acid-base chemistry of g-C$_3$N$_4$ for photocatalytic and catalytic applications.

The authors thank the University of York for financial support (doctoral grant for BC). We thank Dr. Adrian Whitwood for the single crystal X-ray structure determination.

Conflicts of interest

There are no conflicts to declare.

Notes and references

1 a) J.-M. Basset, R. Psaro, D. Roberto and R. Ugo, *Modern Surface Organometallic Chemistry*, Wiley-VCH Verlag GmbH & Co. KGaA, Weinheim, 2009; b) T. Noël, *Organometallic Flow Chemistry*, Springer International Publishing AG, Switzerland, 2016.

2 J. Guzman and B. C. Gates, *Dalton T.*, 2003, DOI: 10.1039/B303285J, 3303-3318.

3 a) W.-J. Ong, L.-L. Tan, Y. H. Ng, S.-T. Yong and S.-P. Chai, *Chem. Rev.*, 2016, **116**, 7159-7329; b) Y. Wang, X. Wang and M. Antonietti, *Angew. Chem. Int. Ed.*, 2012, **51**, 68-89; c) Z. X. Zhou, Y. Y. Zhang, Y. F. Shen, S. Q. Liu and Y. J. Zhang, *Chem. Soc. Rev.*, 2018, **47**, 2298-2321; d) B. Zhu, L. Zhang, B. Cheng and J. Yu, *Appl. Catal B-Environ*, 2018, **224**, 983-999.

4 a) E. Kroke, M. Schwarz, E. Horath-Bordon, P. Kroll, B. Noll and A. D. Norman, *New J. Chem.*, 2002, **26**, 508-512; b) A. Schwarzer, T. Saplinova and E. Kroke, *Coord. Chem. Rev.*, 2013, **257**, 2032-2062; c) B. V. Lotsch, M. Döblinger, J. Sehnert, L. Seyfarth, J. Senker, O. Oeckler and W. Schnick, *Chem. Eur. J.*, 2007, **13**, 4969-4980.

5 a) S.-L. Li, H. Yin, X. Kan, L.-Y. Gan, U. Schwingenschlogl and Y. Zhao, *Phys. Chem. Chem. Phys.*, 2017, **19**, 30069-30077; b) Y. Cao, S. Chen, Q. Luo, H. Yan, Y. Lin, W. Liu, L. Cao, J. Lu, J. Yang, T. Yao and S. Wei, *Angew. Chem. Int. Ed.*, 2017, **56**, 12191-12196; c) S. Hu, F. Li, Z. Fan, F. Wang, Y. Zhao and Z. Lv, *Dalton T.*, 2015, **44**, 1084-1092.

6 a) A. Kumar, P. Kumar, R. Borkar, A. Bansiwal, N. Labhsetwar and S. L. Jain, *Carbon*, 2017, **123**, 371-379; b) H. Kasap, C. A. Caputo, B. C. M. Martindale, R. Godin, V. W. H. Lau, B. V. Lotsch, J. R. Durrant and E. Reisner, *J. Am. Chem. Soc.*, 2016, **138**, 9183-9192; c) R. Kuriki, H. Matsunaga, T. Nakashima, K. Wada, A. Yamakata, O. Ishitani and K. Maeda, *J. Am. Chem. Soc.*, 2016, **138**, 5159-5170; d) R. Kuriki, K. Sekizawa, O. Ishitani and K. Maeda, *Angew. Chem. Int. Ed.*, 2015, **54**, 2406-2409.

7 a) J. Hawecker, J. M. Lehn and R. Ziessel, *J. Chem. Soc., Chem. Commun.*, 1984, 328; b) E. E. Benson, C. P. Kubiak, A. J. Sathrum and J. M. Smieja, *Chem. Soc. Rev.*, 2009, **38**, 89-99.

8 C. Riplinger, M. D. Sampson, A. M. Ritzmann, C. P. Kubiak and E. A. Carter, *J. Am. Chem. Soc.*, 2014, **136**, 16285-16298.

9 a) M. W. George, F. P. A. Johnson, J. R. Westwell, P. M. Hodges and J. J. Turner, *J. Chem. Soc., Dalton Trans.*, 1993, 2977-2979; b) R. W. Balk, D. J. Stufkens and A. Oskam, *J. Chem. Soc., Dalton Trans.*, 1981, 1124-1133.

10 J.-L. Zuo, W.-F. Fu, C.-M. Che and K.-K. Cheung, *Eur. J. Inorg. Chem.*, 2003, **2003**, 255-262.

11 Y. Zhang, J. Liu, G. Wu and W. Chen, *Nanoscale*, 2012, **4**, 5300-5303.

12 a) X. Wang, K. Maeda, A. Thomas, K. Takanabe, G. Xin, J. M. Carlsson, K. Domen and M. Antonietti, *Nat Mater*, 2009, **8**, 76-80; b) S. C. Yan, Z. S. Li and Z. G. Zou, *Langmuir*, 2009, **25**, 10397-10401.

13 J. Martin David, K. Qiu, A. Shevlin Stephen, D. Handoko Albertus, X. Chen, Z. Guo and J. Tang, *Angew. Chem. Int. Ed.*, 2014, **53**, 9240-9245.

14 P. Sundberg, C. Andersson, B. Folkesson and R. Larsson, *J. Electron. Spectrosc. Relat. Phenom.*, 1988, **46**, 85-92.

15 a) S. Oh, J. R. Gallagher, J. T. Miller and Y. Surendranath, *J. Am. Chem. Soc.*, 2016, **138**, 1820-1823; b) Y. Yuan and Y. Iwasawa, *J Phys. Chem. B*, 2002, **106**, 4441-4449; c) M. Komiyama, Y. Ogino, Y. Akai and M. Goto, *J. Chem. Soc. Farad. T. 2*, 1983, **79**, 1719-1728.

16 M. Majumdar, A. Sinha, T. Ghatak, S. K. Patra, N. Sadhukhan, S. M. W. Rahaman and J. K. Bera, *Chem. Eur. J.*, 2010, **16**, 2574-2585.

17 a) S. Saha, M. Kaur and J. K. Bera, *Organometallics*, 2015, **34**, 3047-3054; b) S. Jin and D. Wang, *Acta Crystallogr. E*, 2007, **63**, M3036-U1601; c) S. Jin, D. Wang, Y. Sun and M. Guo, *Acta Crystallogr. E*, 2007, **63**, M3082-U2007; d) S. W. Jin and Y. Sun, *Acta Crystallogr. E*, 2008, **64**, M136-U1321; e) S. W. Jin, Q. J. Zhao, X. G. Qian, R. X. Chen and Y. F. Shi, *Acta Crystallogr. E*, 2008, **64**, M54-U561.

18 M. Majumdar, S. M. W. Rahaman, A. Sinha and J. K. Bera, *Inorg. Chim. Acta*, 2010, **363**, 3078-3087.

19 M. Towrie, A. W. Parker, K. L. Ronayne, K. F. Bowes, J. M. Cole, P. R. Raithby and J. E. Warren, *Appl. Spectrosc.*, 2009, **63**, 57-65.

20 a) A. Vlček, in *Photophysics of Organometallics*, ed. A. J. Lees, Springer Berlin Heidelberg, Berlin, Heidelberg, 2010, pp. 115-158; b) L. A. Worl, R. Duesing, P. Chen, L. D. Ciana and T. J. Meyer, *J. Chem. Soc., Dalton Trans.*, 1991, 849-858.

21 L. Suntrup, S. Klenk, J. Klein, S. Sobottka and B. Sarkar, *Inorg. Chem.*, 2017, **56**, 5771-5783.

22 S. E. Kabir, F. Ahmed, A. Das, M. R. Hassan, D. T. Haworth, S. V. Lindeman, T. A. Siddiquee and D. W. Bennett, *J. Organomet. Chem.*, 2008, **693**, 1696-1702.

23 A. Rostami-Vartooni, V. Mirkhani, H. A. Rudbari and A. J. Moghadam, *Polyhedron*, 2014, **76**, 22-28.

24 R. Costa, N. Barone, C. Gorczycka, E. F. Powers, W. Cupelo, J. Lopez, R. S. Herrick and C. J. Ziegler, *J. Organomet. Chem.*, 2009, **694**, 2163-2170.